A NEW FLAT SHELL FINITE ELEMENT FOR THE LINEAR ANALYSIS OF THIN SHELL STRUCTURES

Djamal Hamadi [a], Ashraf Ayoub [b], and Ounis Abdelhafid [c]

[a, c] Civil Engineering and Hydraulics Department, Faculty of Sciences and Technology, Biskra University, B.P.145, 07000 Biskra – Algeria

[b] Corresponding author; School of Mathematics, Computer Science, and Engineering, City University London, Northampton Square, London EC1V 0HB, UK., Phone: 44(0) 20 7040 8912, Email: Ashraf.Ayoub.1@city.ac.uk

A NEW FLAT SHELL FINITE ELEMENT FOR THE LINEAR ANALYSIS OF THIN SHELL STRUCTURES

Abstract

In this paper, a new rectangular flat shell element denoted 'ACM_RSBE5' is presented. The new element is obtained by superposition of the new strain-based membrane element 'RSBE5' and the well-known plate bending element 'ACM'. The element can be used for the analysis of any type of thin shell structures; even if the geometry is irregular. Comparison with other types of shell elements is performed using a series of standard test problems. A correlation study with an experimentally tested aluminum shell is also conducted. The new shell element proved to have a fast rate of convergence and to provide accurate results.

Keywords: *Flat shell element; thin shell; strain based approach; static condensation.*

1. Introduction

Analytical solutions of practical thin shell structures, particularly those with irregular geometrical shapes, are complex and thus a resort to numerical methods when analyzing them becomes essential. Early work aimed to study shells of revolution in which closed ring shell segments are used [e.g. Jones and Strome, 1966]. The formulation of flat elements [Zienkiewics, 1977] and curved rectangular elements [Corner and Brebbia, 1967] followed. These elements are based on assumed polynomial displacements with linear representation of the in-plane displacements. These elements were found to have a slow rate of convergence, thus the development of high order elements received more attention. Meanwhile, a simple strain-based alternative approach was proposed by Ashwell and Sabir (1972). In this approach, the exact terms representing all rigid body modes and displacement functions corresponding to the element strains are determined by assuming independent strain functions that satisfy the compatibility equations. This approach was used successfully by Sabir and his co-workers (1982, 1985, 1990, 1997) and Mousa and Sabir (1994) to analyze cylindrical, hyperbolic and conical shell structures. These elements in general proved to have a faster convergence rate compared to other models available in the literature. On the other hand, a family of enhanced strain elements, originally developed by Simo and Rifai (1990), were proposed. These include one-point quadrature elements developed by Cardoso et al. (2006, 2008), 4-node exact geometry element proposed by Kulikov and Plotnikova (2010), the improved solid-shell elements of Abed-Meraim and Combescure (2009) using physical stabilization, of Reese (2007) using hourglass stabilization, and of Schwarze and Reese (2009) using reduced integration.

The proposed strain-based approach was also used to develop rectangular and triangular spherical shell elements with five degrees of freedom at each node by Sabir and Djoudi (1998) and Mousa (1992) respectively. These spherical elements were found to produce excellent results with a fast convergence rate. Recently, this approach, also known as the Cardiff Approach, was employed to develop several shell elements, most notably the shallow shell finite element for the analysis of cylindrical shells as well as the cylindrical strain–based shell element for vibration analysis of shell structures developed by Djoudi and Bahai (2003, 2004) respectively. The results of these elements show that efficient convergence can be obtained. More recently, a spherical rectangular finite element based on shallow shell formulation was formulated by Mousa and EL Naggar (2007). This element has six degrees

of freedom at each node and proved to yield accurate results even when using very few finite elements. We note here that most of the above efficient elements are formulated with the appropriate coordinates of the geometrical shape of the structures. Generally, for design purposes, shell structures are constructed with very complicated geometrical shapes and elements, such as folded plates and edge beams. Additional geometrical problems arise, such as when openings, anisotropy, or variation of thickness, are present. However, for practical purposes the flat element approximation gives generally adequate results and permits easy coupling with edge beams and rib members, a capability usually not present in curved element formulations [Zienkiewics and Taylor, 2000]. In flat shell elements, the coupling between membrane and bending action is accounted for at the integration points due to the varying orientation of the element. For practical analysis of shell structures, such flat plate element assumption is typically acceptable, and has the advantage of ease of modeling with reasonable accuracy. Further, because the membrane and bending stresses within an element are decoupled it is easy to understand and control the behaviour of such elements [Hartmann and Kats, 2007]. In this case, the behaviour of a continuously curved surface is represented by a surface made up of small flat elements. Intuitively, as the size of the subdivision decreases it would seem that convergence must occur as discussed by Zienkiewics and Taylor (2000).

In this paper, a new flat shell element is proposed and is denoted as (ACM_ RSBE5). The element is developed by superposition of the new rectangular membrane element R4SBE5 based on the strain approach and the well-known plate bending element ACM discussed in detail in Adini and Clough (1961) and Melosh (1963). The element is characterized by its simplicity compared to existing elements, without compromising its numerical robustness. The stiffness matrix of the new shell element is obtained by combining the two independent membrane and bending stiffness matrices. The displacement field for the strain based membrane element RSBE5 used to construct the flat shell element fully satisfies the equilibrium equations in addition to the compatibility equations. Also, the technique of static condensation of a middle node and the new analytical integration employed in the formulation are the new additions that distinguish this element from other flat shell elements presented in previously published works [e.g. Ashwell and Sabir, 1972; Sabir and Lock, 1972; Belarbi, 2000; Batoz and Dhatt, 1992].

Ashwell and Sabir (1972) developed a cylindrical shell finite element. The element is a rectangular one, having twenty degrees of freedom. It uses only external geometrical nodal displacement, three linear displacements and two rotations; and its formulation is based on strain functions using polar coordinates. The effectiveness of this element has been tested by using it for the analysis of pinched cylinder shell and barrel vault problems. The results showed rapid convergence for displacement. Sabir and Lock (1972) also developed a curved cylindrical shell finite element. They used the standard finite element approach for the formulation adopted by Cantin and Clough (1968), but removed the nodal degrees w_{xy} and included terms containing trigonometrical functions to develop a rectangular cylindrical shell element with 4 nodes and 5 dof/node; which leads to a 20x20 element stiffness matrix. This element is found to converge more rapidly than the Cantin and Clough's model for both symmetrical and unsymmetrical loading conditions. The applications of the elements developed by Sabir and his co-workers are limited to cylindrical shell structures, while the proposed element is a flat shell which can be used for the analysis of general-shape shell structures. The present element contains a middle node to enrich the displacement field that is subsequently condensed out. The element also uses an analytical integration to evaluate the stiffness matrix.

Belarbi (2000) formulated a flat quadrilateral shell element named ACM-SBQ4, obtained by superimposing the standard membrane element SBQ4 with the plate bending element ACM

(Melosh, 1963). The SBQ4 element (Strain Based Quadrilateral element with 4-node) is based on the strain approach, with three degrees of freedom per node including a drilling rotation. The membrane and bending stiffness matrix is obtained by using an analytical integration. This element was examined with three essentials shell tests and the results obtained are compared with those of the proposed 'ACM_RSBE5 in addition to the reference solution. The membrane element SBQ4 contains 4 nodes and 3DOF/node (2 translations and one drilling rotation); but the present element RSBE5 contains 5 nodes: 4 corner nodes and a middle node with 2 translations/node.
Batoz and Dhatt (1992) formulated a set of quadrilateral shell elements based on displacement formulations ; among them Q4γ24 and DKQ24. The first element is based on the Mindlin theory formulation, having four nodes with six degrees of freedom per node and using numerical integration. The second is a flat shell element obtained by superposition of the well-known classical quadrilateral membrane element Q4 and the plate bending element DKQ (Discrete Kirchhoff quadrilateral element with 4 nodes and 3 dof per node). The DKQ24 element is based on Kirchhoff theory with four nodes and six degrees of freedom per node. These two elements are applied to the numerical analysis of Scordelis-Lo (1969) roof test presented in the numerical section in this paper. The results obtained are compared with the reference solutions for both shallow and deep shell theory, in addition to the new formulated element 'ACM_RSBE5' and the flat shell element ACM-SBQ4. We should mention here that the analytical integration technique is used to compute the element stiffness matrices for both elements 'ACM_RSBE5' and ACM-SBQ4. The improved results obtained from the numerical simulations clearly prove the advantages of the proposed element.

In the next section, the formulation of the new element ACM_RSBE5 is presented, followed by standard test problems to evaluate its convergence compared to other quadrilateral shell elements present in the literature. Finally, a correlation study with an experimentally tested elliptical paraboloid shell structure subjected to a uniformly distributed load is presented and the results are discussed.

2. Construction of the New Flat Shell Element ACM_RSBE5

The proposed rectangular shell element is obtained by the superposition of the new formulated element "**RSBE5"** based on the strain approach and described in the next section, and the **ACM** standard plate bending element. The stiffness matrix of the shell element **ACM_ RSBE5** is calculated through analytical integration of the membrane and bending stiffness matrices.

2.1. Formulation of the New Membrane Element "RSBE5"

Figure 1 shows the geometry and nodal displacements of the "**RSBE5"** element (**Rectangular Strain Based Element with 5 nodes)**. The degrees of freedom at each node (i) are denoted U_i and V_i for the horizontal and vertical displacements respectively. The element was developed by Hamadi (2006) and has four nodes at the corner in addition to an internal node, each having two degrees of freedom (d.o.f). Through the introduction of an additional internal node, the element has proven to be more accurate, even though it requires static condensation following the approach of Bathe and Wilson (1976).

[Fig. 1]

The strain components at any point in the Cartesian coordinate system are expressed in terms of the displacements U and V as follow:

$$\varepsilon_x = U_{,x} \qquad (1a)$$

$$\varepsilon_y = V,_y \tag{1b}$$

$$\gamma_{xy} = U,_y + V,_x \tag{1c}$$

If the strains given by equations (1) are equal to zero, the integration of equations (1) leads to expressions of the form:

$$U = a_1 - a_3 y \tag{2a}$$

$$V = a_2 + a_3 x \tag{2b}$$

Equations (2) represent the displacement field in terms of its three rigid body displacements. The strains in equation (1) cannot be considered independent since they must satisfy the compatibility equation. This equation can be obtained by eliminating U, V from equation (1), hence:

$$\frac{\partial^2 \varepsilon_x}{\partial y^2} + \frac{\partial^2 \varepsilon_y}{\partial x^2} - \frac{\partial^2 \gamma_{xy}}{\partial x \partial y} = 0 \tag{3}$$

Equation (2) represents the three components of the rigid body displacements through three independent constants (a_1, a_2, a_3). Thus seven additional constants (a_4, $a_5 \ldots a_{10}$) are needed to express the displacements due to straining of the element. These seven independent constants are used to describe the strains as follow:

$$\begin{cases} \varepsilon_x = a_4 + a_5 y + a_9 x \\ \varepsilon_y = a_6 + a_7 x + a_{10} y \\ \gamma_{xy} = -a_5 x R - a_7 y R + a_8 - a_9 H y - a_{10} H x \end{cases} \tag{4}$$

With: $H = \dfrac{2}{(1-\nu)}$; $R = \dfrac{2\nu}{(1-\nu)}$

The strains given by equations (4) satisfy both the compatibility equation (3) and the two-dimensional equilibrium equations (5a) and (5b):

$$\frac{\partial \sigma_x}{\partial x} + \frac{\partial \tau_{xy}}{\partial y} = 0 \tag{5a}$$

$$\frac{\partial \sigma_y}{\partial y} + \frac{\partial \tau_{xy}}{\partial x} = 0 \tag{5b}$$

By integrating equations (4), the displacements are evaluated as follow:

$$U = a_4 x + a_5 xy - a_7 y^2 (R+1)/2 + a_8 y/2 + a_9 (x^2 - H y^2)/2 \tag{6a}$$

$$V = -a_5 x^2 (R+1)/2 + a_6 y + a_7 xy + a_8 x/2 + a_{10} (y^2 - H x^2)/2 \tag{6b}$$

By adding equations (2) and (6); the final displacements representing rigid body modes and straining actions are evaluated as follow:

$$\begin{cases} U = a_1 - a_3 y + a_4 x + a_5 xy - a_7 \dfrac{y^2 (R+1)}{2} + a_8 \dfrac{y}{2} + a_9 \dfrac{1}{2}(x^2 - Hy^2) \\ V = a_2 + a_3 x - a_5 \dfrac{x^2 (R+1)}{2} + a_6 y + a_7 xy + a_8 \dfrac{x}{2} + a_{10} \dfrac{1}{2}(y^2 - Hx^2) \end{cases} \quad (7)$$

The stiffness matrix is then calculated from the well-known expression:

$$[K_e] = [A^{-1}]^T [K_0] [A^{-1}] \quad (8a)$$

where $$[K_0] = \iint_S [Q]^T [D][Q] dx.dy \quad (8b)$$

and

$$[Q] = \begin{bmatrix} 0 & 0 & 0 & 1 & y & 0 & 0 & 0 & x & 0 \\ 0 & 0 & 0 & 0 & 0 & 1 & x & 0 & 0 & y \\ 0 & 0 & 0 & 0 & -xR & 0 & -yR & 1 & -Hy & -Hx \end{bmatrix} \quad (9)$$

$$[D] = \begin{bmatrix} D11 & D12 & 0 \\ D12 & D22 & 0 \\ 0 & 0 & D33 \end{bmatrix}$$ is the usual constitutive matrix

$$D11 = D22 = \frac{E}{(1-\nu^2)} \; ; \; D12 = \frac{\nu.E}{(1-\nu^2)} \; ; \; D33 = \frac{E}{2(1+\nu)}$$

For [A] and [K_0] see Appendices *A* and *B.*

At the end of the state determination, the 2 additional middle dofs are condensed out. The evaluation of the integral in Eq. (8b) follows the approach of Hamadi and Belarbi (2006) using an exact and not reduced analytical integration. Such an approach resolves numerical problems associated with geometrical distortions of the element.

2.2. Rectangular Plate Element 'ACM'

The displacement fields of the **ACM** element (Fig.2) are given by the following expressions:

[Fig. 2]

$$\begin{aligned} W(x,y) &= a_1 + a_2 x + a_3 y + a_4 x^2 + a_5 xy + a_6 y^2 + a_7 x^3 + a_8 x^2 y \\ &\quad + a_9 xy^2 + a_{10} y^3 + a_{11} x^3 y + a_{12} xy^3 \\ \theta_x &= -(a3 + a_5 x + 2 a_6 y + a_8 x^2 + 2a_9 xy + 3 a_{10} y^2 + a_{11} x^3 + 3 a_{12} xy^2) \\ \theta_y &= a_2 + 2a_4 x + a_5 y + 3a_7 x^2 + 2a_8 xy + a_9 y^2 + 3 a_{11} x^2 y + a_{12} y^3 \end{aligned} \quad (10)$$

The shell element **ACM_RSBE5** (Fig.3c) is obtained by superposition of the two elements RSBE5 and ACM in the following manner:

(a) + (b) = (c)

[Fig. 3]

3. Numerical Tests

The performance of the formulated flat shell element is evaluated using the following popular test problems:

3.1. Clamped Cylindrical Shell

In this test problem, a clamped cylindrical shell (Fig.4 a) is evaluated. This test of thin shells (R/h=100) is considered by many researchers as a severe test. It makes it possible to examine the aptitude of shell elements to simulate complicated membrane state problems dominated by bending. The dimensions, material properties, and loading conditions are shown in Fig.4. Due to symmetry, only 1/8 of the shell (region ABCD) is considered in the finite element idealisation (Fig.4 b).

[Fig. 4]

The results obtained for different meshes for both, the proposed ACM_RSBE5 and the ACM_SBQ4 of Belarbi (2000), are presented in Tables 1 and 2.

[Tables 1-2]

The numerical results are compared to the analytical solution based on thin shell theories (R/h=100), and given below by Flugge and Fosberge (1966) and Lindberg et al. (1969):

$W_C = -W_C\ Eh/P = 164.24$ deflection under load P at point C only

$V_D = -V_D\ Eh/P = 4.11$ deflection in the Y direction

Table 1 also summarizes the solution time used in the analysis of the clamped cylindrical shell with different meshes. The processor machine used has the following properties: Intel(R) Core(TM) i3-2330M CPU@2.2 GHZ RAM: 4.00Go

The results obtained by the present element ACM_RSBE5 for the vertical displacement at point C (normalized values) are slightly better than those given by the element ACM-SBQ4, and much better than those of the hexahedral element HEX20, the standard full-integration solid element reported in Abed-Meraim et al. (2013). It also performs better than the 6-node solid-shell element SHB6 (Abed-Meraim et al., 2012), and the 8-node solid-shell element SHB8PS (Abed-Meraim and Combescure, 2007) [Table 1]. It performs relatively better than the widely used Reduced integration Enhanced strain Solid-Shell (RESS) element developed by Alves de Souza et al. (2005) [Table 1]. It significantly converges more rapidly than both, the standard prismatic elements PRI15 and the solid-shell prismatic element SHB15 developed by Abed-Meraim et al. (2013); for example for meshes (10x10) the results for these elements are 0.625 and 0.646 respectively, but for the ACM_RSBE5 are 0.955 for a mesh of 8x8 elements only. Even when compared with higher order elements, such as the 20-node solid shell element SHB20 developed by Abed-Meraim

et al. (2013), its performance is relatively good (0.955 as opposed to 0.979 for a mesh of 8x8).

The results obtained for both deflections W_C and V_D for the refined mesh (20x4) of the proposed element are in good agreement with the analytical solution.

Figures 5 and 6 show the convergence curves for the results obtained from elements **ACM_RSBE5** and ACM-SBQ4 for the deflections at points C and D. From the above figures, it is concluded that the **ACM_RSBE5** has a good convergence rate.

[Figs. 5-6]

3.2. Scordelis-Lo Roof

In the next test problem, the Scordelis-Lo (1969) roof is considered. The roof structure has the geometry shown in Fig.7. The straight edges are free, while the curved edges are supported on rigid diaphragms along their plane. The geometry and material properties are given in Fig.7. Considering the symmetry of the problem, only one quarter of the roof is analysed (part ABCD). The results obtained using the proposed element **ACM_RSBE5** are compared to the reference values based on the deep shell theory.

[Fig. 7]

The analytical solution based on the shallow shell theory is given by Scordelis and Lo (1969), which is slightly different from the deep shell theory. The convergence curves are presented in Figs.8 and 9 for the vertical displacement at the midpoint B of the free edge and the center C of the roof.

[Figs. 8-9]

The results are also compared to several other quadrilateral shell elements, namely Q4γ24, DKQ24 presented by Batoz and Dhatt (1992) and ACM-SBQ4 developed by Belarbi (2000). Figures 8, 9, 10, and 11 show the convergence curve for the deflections Wc at point C and W_B at point B obtained from the quadrilateral shell elements cited above.

The above results confirm the good convergence of the new formulated shell element **ACM_RSBE5.**

[Figs. 8-11]

3.3. Pinched Cylinder with Free Edges

The pinched cylinder shown in Fig. 12 is one of the most common examples used in the literature to test shell elements. Indeed, since 1967 this example served as a test problem to assess the performance of new axisymmetric shell elements regarding the rapidity of convergence and especially the representation of rigid body modes. By reason of symmetry, only one-eighth of the cylinder is modeled. The symmetry conditions are imposed along AB, AD and DC (Fig.12). Two cases of cylinder thickness and applied loads are considered (h_1, F_1 and h_2, F_2).

[Fig. 12]

One-eighth of the cylinder is modeled with different meshes, and the normal displacement W_C at point C is calculated. The convergence of the new element **ACM_RSBE5** is compared

with the analytical solution (deep shells theory) and with other elements available in the literature; these are models: BOG (Bogner et al. 1967); CAN68 (Cantin and Clough, 1968); ASH72 (Ashwell and Sabir, 1972); and SAB72 (Sabir and Lock, 1972). The results obtained are presented in Tables 3 and 4, and the convergence curves for different elements are shown in Figs. 13 and 14.

[Tables 3-4]

[Figs. 13-14]

The results obtained and presented in Tables 3, 4 and Figs. 13 and 14 confirm the excellent performance of the formulated element ACM_RSBE5. The ACM_RSBE5 converges to deep shell solutions (to WC = - 0.1139 m for h = 0.094m and F= 100 and from WC = - 0.02439 m h = 0.01548 m) with only a few elements (9 elements for the first case and 3 elements for the second case), contrarily to the other elements and slightly better than ACM_SBQ4.

4. Experimental Investigation

A correlation study with an experimentally tested shell structure is conducted. The shell is assumed to be constructed from a perfectly elastic material. Tests on full-scale shell structures are scarce due to the associated high cost; hence the experimental work described in this study is for a small-scale specimen. The test details are described next.

4.1. Description of the Elliptical Paraboloid Shell Model (Fig.15)

The equation for the surface is written in the following manner as discussed by Beles and Soare (1975):

$$Z_1 = 4 f_x \frac{x^2}{l_x^2} + 4 f_y \frac{y^2}{l_y^2} \tag{11a}$$

$$Z_2 = 4 f_x \frac{x(x-l_x)}{l_x^2} + 4 f_y \frac{y(y-l_y)}{l_y^2} \tag{11b}$$

$$Z_3 = f_x \left(\frac{2x}{l_x} - 1 \right)^2 + 4 f_y \frac{y^2}{l_y^2} \tag{11c}$$

[Fig. 15]

The elliptical shape specimen is made of an aluminum alloy and has a constant thickness of 2 mm with a rectangular projection of 880 mm by 400 mm (Fig. 16). The material properties used are: The modulus of elasticity E = 70000 N/mm^2, the Poisson ratio υ = 0.33. The shell is free along the long edges, and fixed on a wooden support along the short edges. Due to the double symmetry in geometry and loading, the measuring points are located on one quarter of the area of the model, at the eight points shown in Fig.17.

Eight deflections gauges capable of measuring displacements perpendicular to the surface of the shell are located under the shell. A further two deflection gauges are mounted to check for symmetry (Fig.17).

[Figs. 16-17]

4.2. Loading

A uniform normal pressure is applied by covering the shell top surface with a pneumatic pressure bag. Four different values of loading are applied, 10, 20, 30, and 40 cm of water (in which 1 cm of water = 0.0142233 lb/ in^2 equivalent to $2.5x10^{-3}$ N/mm^2).

4.3 Numerical and Experimental Results

A mesh of 16x8 elements is used for the numerical analysis. The experimental and analytically computed vertical deflections for the different loading levels are presented in Table 5.

[Table 5]

4.4. Comparison between Theoretical and Experimental Results

In elastic analysis, as the loading was doubled, the deflections were doubled. This was not the case in the experimental work. This is due to a few points which could be explained as follows:

One of the main problems with the experiment was the lack of uniformity of the distributed load. The air-filled bag did not evenly distribute the pressure because loads measured at the four corners were found to be slightly different.

A further probable cause of inaccuracy was the positioning of the deflection gauges. The problem was to ensure that the gauges were perpendicular to the shell surface. Although this was easy to achieve in the central position (since it is horizontal), this was note so easily achieved near the edges where the shell surface is considerably angled.

In addition to the various experimental inaccuracies, in the theoretical analysis non deflecting support conditions are assumed, which is not strictly the case in the experiments. Finally, differences may results from other considerations. However, in general the results obtained from the finite element analysis are in reasonable agreement with those measured experimentally.

5. Conclusion

A new strain-based element denoted ACM_RSBE5 is proposed. The element combines the new RSBE5 strain-based membrane model with the classical ACM plate model. A series of test problems were conducted to evaluate the efficiency of the element compared to other elements in the literature. The results obtained confirmed the fast convergence rate of the element. Further, a correlation study with an experimentally tested aluminum shell structure confirmed the accuracy of the proposed element, in particular in predicting the displacements of the inside points. The proposed element has the advantage of being simple in form and uses only the five essential degrees of freedom. Further, it can be used for the analysis of thin shell structures, even those with complex geometries. The current formulation is for linear analysis, but extension to account for both geometric and material nonlinearities is the subject of an ongoing investigation that will be published in future work.

References

Abed-Meraim, F., and Combescure, A. (2007). A physically stabilized and locking-free formulation of the SHB8PS solid–shell element. *European Journal of Computational Mechanics* 16(8):1037–1072.

Abed–Meraim, F., Comberscure, A. (2009). An Improved Assumed Strain Solid shell Element Formulation with Physical Stabilization for Geometric Non–linear Applications and Elastic-plastic Stability Analysis. *Int. Journal for Numerical Methods in Eng.,* 80, 1640–1686.

Abed-Meraim, F., Trinh, V., and Combescure, A. (2012). Assumed strain solid–shell formulation for the six-node finite element SHB6: evaluation on non-linear benchmark problems, *European Journal of Computational Mechanics,* 21:1-2, 52-71.

Abed-Meraim, F., Trinh, V., and Combescure, A. (2013). New quadratic solid–shell elements and their evaluation on linear benchmark problems. *Computing* 95:373–394.

Adini A. and Clough R.W. (1961). Analysis of plate bending by the finite element method. Report to the Nat. Sci. Found., U.S.A., G 7337.

Alves de Souza, R.J., Cardoso, R.P.R., Fontes Valente, R.A, Yoon, J.W., Gracio, J.J., and Jorge, R.M.N. (2005). A new one-point quadrature enhanced assumed strain (EAS) solid-shell element with multiple integration points along thickness: Part I—geometrically linear applications. *Int. Journal for Numerical Methods in Eng.*, 62, 952–977.

Ashwell, D.G. and Sabir, A.B. (1972). A new cylindrical shell finite element based on simple independent strain functions. Int. J. Mech. Sci.; (14): 171-183.

Bathe K.J. and Wilson E.L. (1976). Numerical Methods in finite element analysis. Prentice Hall, New Jersey.

Batoz J.L., and Dhatt G. (1992). Modélisation des structures par éléments finis, Vol. 3 : coques, Eds Hermès, Paris.

Belarbi M.T. (2000). Développement de nouveaux éléments finis basés sur le modèle en déformation. Application linéaire et non linéaire. Thèse de Doctorat d'état, Université de Constantine, Algérie.

Beles, A. A. Soare, M. V. (1975). Elliptic and Hyperbolic Paraboloidal Shells Used in Construction. Bucharest, 145-146.

Bogner F.K., Fox R.L. and Schmit L.A. (1967). A cylindrical Shell Discrete Element, AIAA Journal, Vol. 5, N° 4, pp. 745-750.

Cantin G. and Clouth R.W. (1968). A curved cylindrical shell Finite Element, AIAA Journal, Vol. 6, N° 6, pp. 1057-1062.

Cardoso, R.P.R., Yoon, J.W., and Fontes Valente, R.A. (2006). A New Approach to Reduce Membrane and Transverse Shear Locking for One-point Quadrature Shell Elements: Linear Formulation. *Int. Journal for Numerical Methods in Eng.*, 66, 214–249.

Cardoso, R.P., Yoon, J.W., Mahardika, M., Choudhry, S., Alves de Sousa, R.J., and Fontes Valente, R.A. (2008). Enhanced Assumed Strain (EAS) and Assumed Natural Strain (ANS) Methods for One-point Quadrature Solid–shell Elements. *Int. Journal for Numerical Methods in Eng.,* 75, 156–187.

Corner JJ, Brebbia C. (1967). Stiffness matrix for shallow rectangular shell element. *J. Eng. Mech., ASCE,* 93(EM5): 43-65.

Djoudi, M.S and Bahai, H. (2003). A shallow shell finite element for linear and non-linear analysis of cylindrical shells. *Engineering Structures,* (25): 769-778.

Djoudi, M.S and Bahai, H. (2004). A cylindrical strain- based shell element for vibration analysis of shell structures. *Finite Element in Analysis and Design*, (40): 1947-1961.

Flugge W. and Fosberge K. (1966). Point load on shallow elliptic paraboloid. *J. Appl. Mech.,* (33): 575-585.

Hamadi, D. (2006). "Analysis of structures by non-conforming finite elements. PhD Thesis, Civil Engineering Department, Biskra University, Algeria, pp. 130.

Hamadi, D. and Belarbi, M.T. (2006). Integration solution routine to evaluate the element stiffness matrix for distorted shapes. Asian Journal of Civil Engineering (Building and Housing), 7(5): 525 -549.

Hartmann F. and Kats C. (2007). Analysis with finite element methods. Springer.

Jones RE, Strome DR. (1966). Direct stiffness method analysis of shells of revolution utilizing curved elements. *AIAA.J*, 4(9): 1519-25.

Kulikov, G.M., Plotnikova, S.V. (2010). A Family of ANS Four–node Exact Geometry Shell Elements in General Convected Curvilinear Coordinates. *Int. Journal for Numerical Methods in Eng.*, 83, 1367–1406.

Lindberg G.M., Olson M.D. and Cowper G.R. (1969). New development in the finite element analysis of shells. Q. Bull Div. Mech. Eng. and Nat. Aeronautical Establishment, National Research council of Canada, Vol. 4.

Melosh R.J., (1963). Basis of derivation of matrices for the direct stiffness method. *J.AIAA*, 1(N7): 1631-1637.

Mousa, A.I. and Sabir, A.B. (1994). Finite element analysis of fluted conical shell roof structures. Computational Structural Engineering in Practice, Civil Comp. press- ISRN O-948 748- 30x: 173-181.

Mousa, A.I. (1992). Triangular finite element for analysis of spherical shell structures. UWCC Publications, Internal Report, University of Wales, college Cardiff, U.K.

Mousa A.I and EL Naggar, M.H. (2007). Shallow Spherical Shell Rectangular Finite Element for Analysis of Cross Shaped Shell Roof. *Electronic Journal of Structural Engineering*, (7): 769-778.

Reese, S. (2007). A Large Deformation Solid–shell Concept Based on Reduced Integration with Hourglass Stabilization. *Int. Journal for Numerical Methods in Eng.*, 69, 1671–1716.

Sabir A.B. and Lock A.C. (1972). A curved cylindrical shell finite element, IJMS. Vol. 14, pp. 125-135.

Sabir, A.B and Charchaechi, T.A. (1982). Curved rectangular and general quadrilateral shell finite elements for cylindrical shells. The Math of Finite Element and Appli., IV Academic Press: 231-239.

Sabir, A.B and Ramadhani, F. (1985). A shallow shell finite element for general shell analysis. Variation Method in Engineering, Proceedings of the 2nd International Conference, University of Southampton, England.

Sabir, A.B and Djoudi, M.S. (1990). A shallow shell triangular finite element for the analysis of hyperbolic parabolic shell roof. FEMCAD. Struct. Eng. and Optimization: 49-54.

Sabir, A.B. (1997). Strain based shallow spherical shell element. Proc. Int. Conf on the Math. Finite elements and application, Brunel University, England.

Sabir, A.B and Djoudi, M.S. (1998). A shallow shell triangular finite element for the analysis of spherical shells. *Structural Analysis J.*: 51-57.

Scordelis A.C. and Lo K.S. (1969). Computer analysis of cylindrical shells. *J. Amer. Concrete Institute*, (61): 539-561.

Simo, J.C. Rifai, M.S. (1990). A Class of Mixed Assumed Strain Methods and the Method of Incompatible Modes. *Int. Journal for Numerical Methods in Eng.*, 29, 1595–1638.

Schwarze, M., Reese, S. (2009). A Reduced Integration Solid–shell Finite Element Based on the EAS and the ANS Concept—Geometrically Linear Problems. *Int. Journal for Numerical Methods in Eng.*, 80, 1322–1355.

Zienkiewics O.C. (1977). The finite element method. 3rd ed". London: McGraw Hill.

Zienkiewics O.C. and Taylor, R.L. (2000). The finite element method, Vol. Solid Mechanics.5th ed. Butterworth –Heinemann.

Notations

a_i Constants in displacement fields

$[A]$ Transformation matrix

$[D]$ Rigidity matrix

E, v Young's modulus and Poisson's ratio, respectively

h Shell thickness

$[K_e]$ Stiffness matrix

L Shell length

$[Q]$ Strain matrix

R Radius of the shell

U, V In plane displacement in x and y, respectively

W Normal displacement

X, Y Cartesian coordinates

θ_x, θ_y and θz rotations about x, y and z axes respectively

ε_x, εy Direct strains in the x and y directions

γ_{xy} Membrane shear strain

Appendices

Appendix A

$$[A]=\begin{bmatrix}
1 & 0 & 0 & 0 & 0 & 0 & 0 & 0 & 0 & 0 \\
0 & 1 & 0 & 0 & 0 & 0 & 0 & 0 & 0 & 0 \\
1 & 0 & 0 & a & 0 & 0 & 0 & 0 & \frac{a^2}{2} & 0 \\
0 & 1 & a & 0 & \frac{-a^2(R+1)}{2} & 0 & 0 & \frac{a}{2} & 0 & \frac{-Ha^2}{2} \\
1 & 0 & -b & a & ab & 0 & \frac{-b^2(R+1)}{2} & \frac{b}{2} & \frac{a^2-Hb^2}{2} & 0 \\
0 & 1 & a & 0 & \frac{-a^2(R+1)}{2} & b & ab & \frac{a}{2} & 0 & \frac{b^2-Ha^2}{2} \\
1 & 0 & -b & 0 & 0 & 0 & \frac{-b^2(R+1)}{2} & \frac{b}{2} & \frac{-Hb^2}{2} & 0 \\
0 & 1 & 0 & 0 & 0 & b & 0 & 0 & 0 & \frac{b^2}{2} \\
1 & 0 & -\frac{b}{2} & \frac{a}{2} & \frac{ab}{4} & 0 & -\frac{b^2}{8}(R+1) & \frac{b}{4} & \frac{a^2-Hb^2}{8} & 0 \\
0 & 1 & \frac{a}{2} & 0 & -\frac{a^2}{8}(R+1) & \frac{b}{2} & \frac{ab}{4} & \frac{a}{4} & 0 & \frac{b^2-Ha^2}{8}
\end{bmatrix}$$

Appendix B

$$[K_0]=\begin{bmatrix}
0 & 0 & 0 & 0 & 0 & 0 & 0 & 0 & 0 & 0 \\
 & 0 & 0 & 0 & 0 & 0 & 0 & 0 & 0 & 0 \\
 & & 0 & 0 & 0 & 0 & 0 & 0 & 0 & 0 \\
 & & & H_1 & H_2 & H_3 & H_4 & 0 & H_5 & H_6 \\
 & & & & H_7 & H_8 & H_9 & H_{10} & H_{11} & H_{12} \\
 & & & & & H_{13} & H_{14} & 0 & H_{15} & H_{16} \\
 & & & & & & H_{17} & H_{18} & H_{19} & H_{20} \\
 & & & & & & & H_{21} & H_{22} & H_{23} \\
 & & & & & & & & H_{24} & H_{25} \\
 & & & & & & & & & H_{26}
\end{bmatrix}$$

$$H_1 = abD_{11}$$

$$H_2 = \frac{1}{2}ab^2D_{11}$$

$$H_3 = abD_{12}$$

$$H_4 = \frac{1}{2}ba^2D_{12}$$

$$H_5 = \frac{1}{2}ba^2D_{11}$$

$$H_6 = \frac{1}{2}ab^2D_{12}$$

$$H_7 = \frac{1}{3}\left(ab^3D_{11} + ba^3R^2D_{33}\right)$$

$$H_8 = \frac{1}{2}ab^2D_{12}$$

$$H_9 = \frac{a^2b^2}{4}\left(R^2D_{33} + D_{12}\right)$$

$$H_{10} = -\frac{1}{2}Rba^2D_{33}$$

$$H_{11} = \frac{a^2b^2}{4}\left(RHD_{33} + D_{11}\right)$$

$$H_{12} = \frac{1}{3}\left(ab^3D_{12} + ba^3RHD_{33}\right)$$

$$H_{13} = abD_{22}$$

$$H_{14} = \frac{1}{2}ba^2D_{22}$$

$$H_{15} = \frac{1}{2}ba^2D_{12}$$

$$H_{16} = \frac{1}{2}ab^2D_{22}$$

$$H_{17} = \frac{1}{3}\left(ba^3D_{22} + ab^3R^2D_{33}\right)$$

$$H_{18} = -\frac{1}{2}ab^2RD_{33}$$

$$H_{19} = \frac{1}{3}\left(ba^3D_{12} + ab^3RHD_{33}\right)$$

$$H_{20} = \frac{a^2b^2}{4}\left(RHD_{33} + D_{22}\right)$$

$$H_{21} = abD_{33}$$

$$H_{22} = -\frac{1}{2}ab^2HD_{33}$$

$$H_{23} = -\frac{1}{2}ba^2HD_{33}$$

$$H_{24} = \frac{1}{3}\left(ab^3H^2D_{33} + ba^3D_{11}\right)$$

$$H_{25} = \frac{a^2b^2}{4}\left(H^2D_{33} + D_{12}\right)$$

$$H_{26} = \frac{1}{3}\left(ba^3H^2D_{33} + ab^3D_{22}\right)$$

Where: $D11 = D22 = \frac{E}{\left(1-\nu^2\right)}$; $D12 = \frac{\nu.E}{\left(1-\nu^2\right)}$; $D33 = \frac{E}{2\left(1+\nu\right)}$;

With: $H = \frac{2}{\left(1-\nu\right)}$; $R = \frac{2\nu}{\left(1-\nu\right)}$

Table Caption

Figure Caption

Table 1 Clamped cylindrical shell, convergence of W_C (normalized values)

Meshes	Displacement Wc at point C					Solution time (Sec) **ACM_RSBE5**
	ACM_RSBE 5	**ACM-SBQ4**	**HEX20**	**SHB8PS**	**RESS**	
4 x 4	0.649	0.618	0.140	0.387	0.112	0.10000
6 x 6	0.842	0.821	0.328			0.17999
8 x 8	0.955	0.904	0.523	0.754	0.59	0.26999
20 x 4	0.984	0.956	0.675			0.28845
16x16				0.94	0.933	
Analytical solution	**164.24 (1.00 Normalized results)**					

Table 2 Clamped cylindrical shell, convergence of V_D

Meshes	Displacement V_D at point D	
	ACM_RSBE5	**ACM-SBQ4**
4 x 4	6.206	6.153
6 x 6	4.837	4.809
8 x 8	4.521	4.274
20 x 4	4.179	4.192
Analytical solution	**4.11**	

Table 3: Pinched Cylinder with free edges, convergence of W_C

Case 1: P_1=100; h_1=0,094 m; L=10,35 m ; R=4,953 m ; E=10,5x10^6; ν=0,3125

Meshes	W_C					Solution time (Seconds) **ACM_RSBE5**
	[Bog 67) [29]	[CAN 68] with RBM [30]	[CAN 68] without RBM [30]	ACM_SBQ4 [19]	**ACM_RSBE5**	
1x1	0.0025	-	-	0.0860	0.08763	0.006999
1x3	0.1026	0.0297	0.0009	0.1041	0.1060	0.016999
1x4	0.1087	-	-	-	0.1100	0.026000
1x5	-	0.0769	0.0021	0.1090	0.1116	0.043998
1x7	-	0.0987	0.0035	0.1102	0.1129	0.049998
1x8	-	-	-	-	0.1132	0.052000
1x9		0.1057	0.0051	0.1115	0.1134	0.054000
Exact solution	**0.1139**					

Table 4: Pinched Cylinder with free edges, convergence of W_C
Case 2: $P_2 = 0,1$; $h_2 = 0,01548$ m; L=10,35 m ; R=4,953 m ; $E=10,5x10^6$; $\nu=0,3125$

Meshes	W_C					Solution time (Seconds) for **ACM_RSBE5**
	[ASH 72] [4]	[CAN 68] [30]	[SAB 72] [23]	ACM_SBQ4 [19]	**ACM_RSBE5**	
1x1	0.02301	0.00001	0.00001	0.01922	0.0196	0.0000
1x3	0.02302	0.00001	0.00001	0.02302	0.02343	0.00999
1x4	0.02403	0.00074	0.00063	-	-	
1x5	-	-	-	0.02387	-	
1x7	-	-	-	0.02418	-	
2x4	0.02409	0.00070	0.00064	-	-	
3x4	0.02414	0.00068	0.00065	-	-	
Exact solution	**0.02439**					

Table 5 Vertical Displacements W (mm) Under Different Applied Loadings

Case a Load $=25x10^{-3}$ N/mm^2	Points	3	4	5	6	7	8
	ACM_RSBE5	0.24	0.40	2.01	0.16	0.25	0.41
	Exp.Work	0.19	0.31	1.67	0.13	0.18	0.30
Case b Load $=50x10^{-3}$ N/mm^2	ACM_ RSBE5	0.48	0.80	4.02	0.32	0.50	0.82
	Exp.Work	0.49	0.80	3.10	0.33	0.47	0.85
Case c Load $=75x10^{-3}$ N/mm^2	ACM_ RSBE5	0.72	1.20	6.03	0.48	0.75	1.23
	Exp.Work	0.66	1.09	5.20	0.43	0.63	1.15
Case d Load $=100x10^{-3}$ N/mm^2	ACM_ RSBE5	0.96	1.60	8.02	0.65	1.00	1.64
	Exp.Work	1.04	1.70	7.70	0.68	1.00	1.90

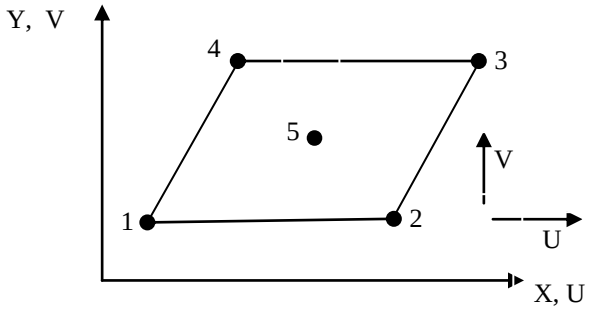

Fig.1. Co-ordinates and nodal points for the rectangular element" RSBE5"

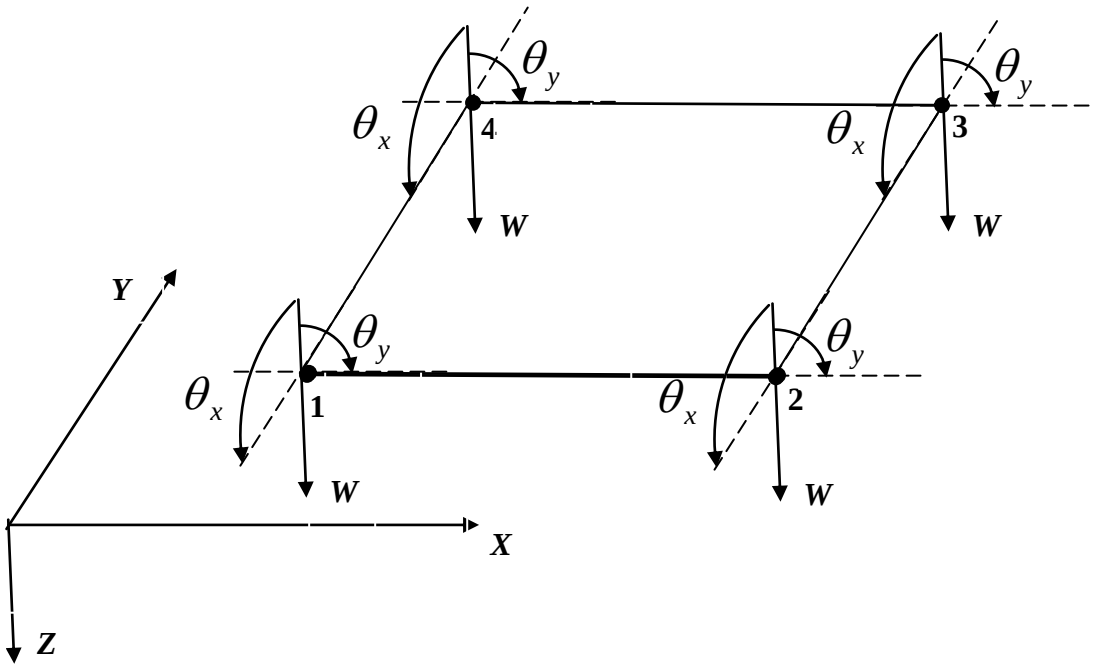

Fig.2. Co-ordinates and nodal points for the rectangular plate element" ACM"

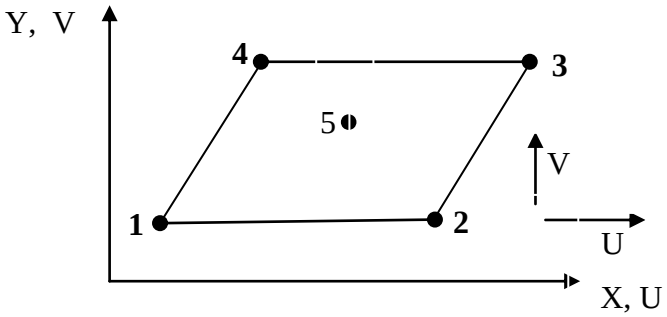

RSBE5

+

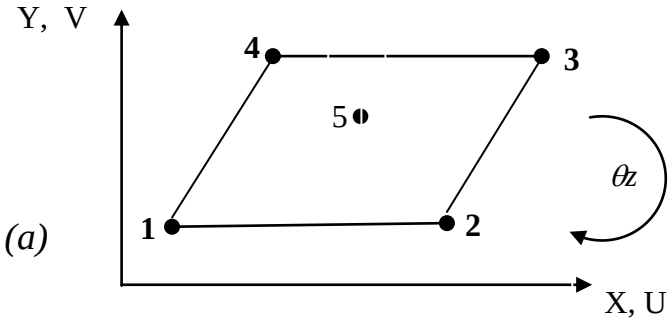

(a)

Fictive rotation θz

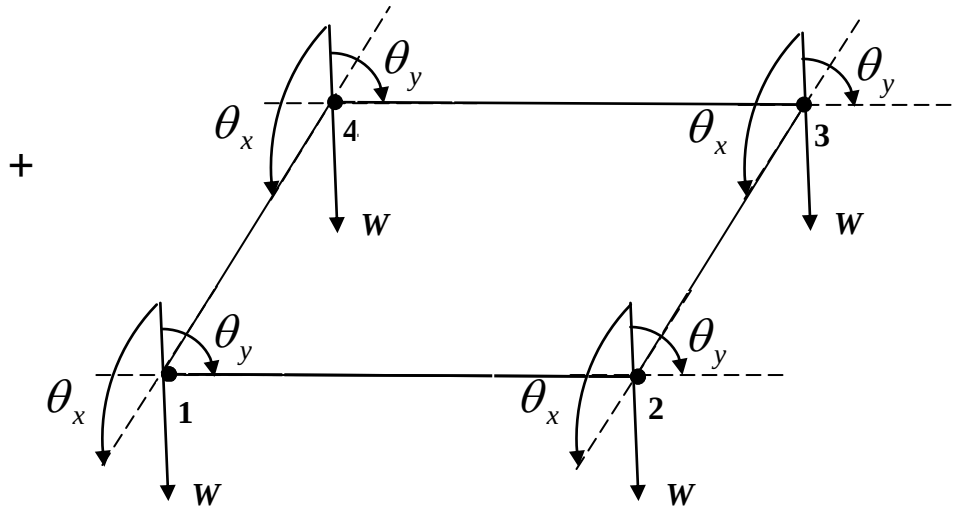

(b) ACM

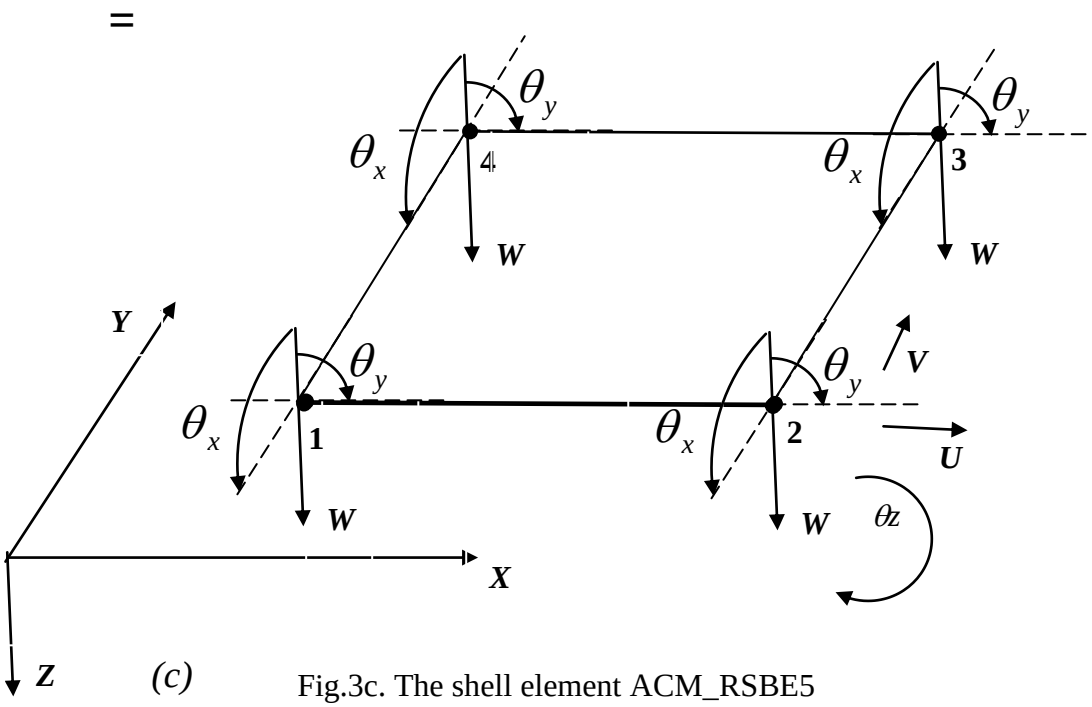

(c) Fig.3c. The shell element ACM_RSBE5

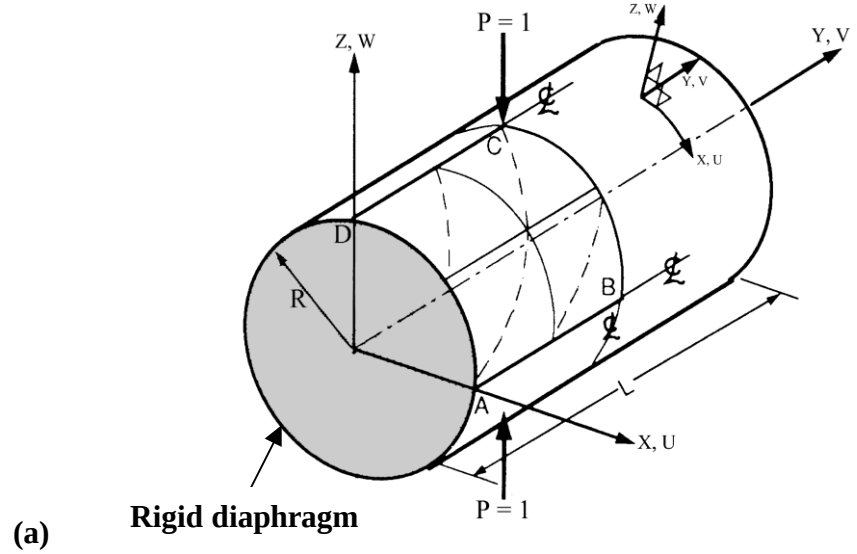

(a) **Rigid diaphragm**

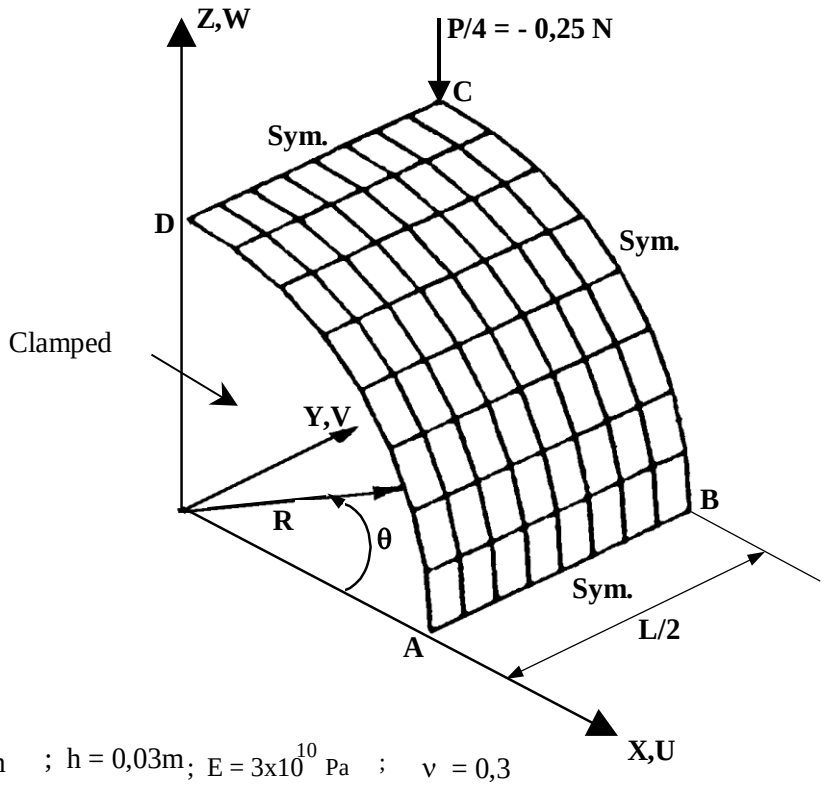

(b)

Data:

L=6 ; R=3m ; h = 0,03m; $E = 3x10^{10}$ Pa ; $\nu = 0,3$

Symmetry conditions:

$\mathbf{W} = \theta_Y = \theta_X = 0$ at AB
$\mathbf{V} = \theta_X = \theta_Z = 0$ at BC
$\mathbf{U} = \theta_Y = \theta_Z = 0$ at CD

Boundary conditions:

$U = W = \theta_Y = 0$ at AD

Fig.4. Clamped cylindrical shell

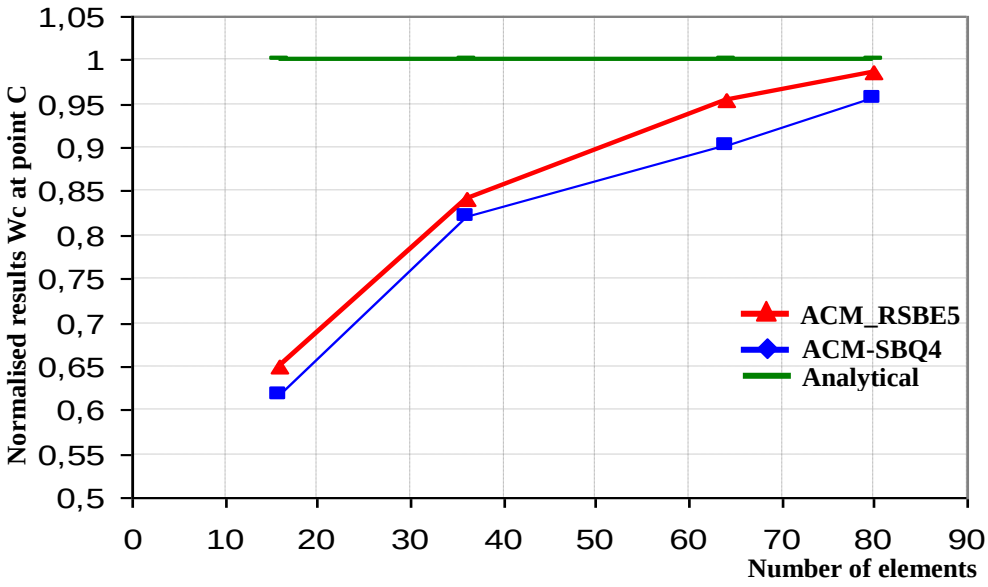

Fig.5. Convergence curve for the deflection Wc at point C

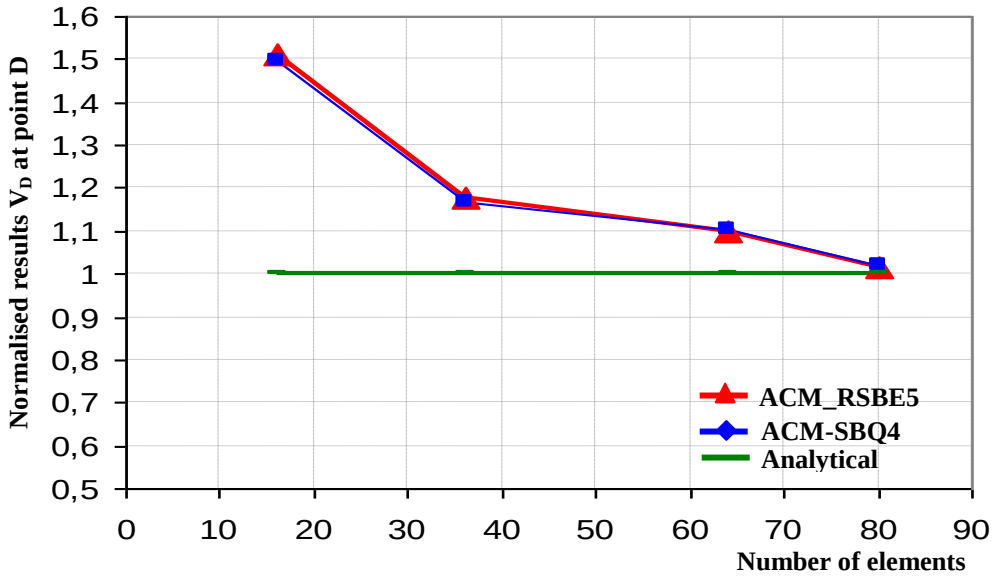

Fig.6. Convergence curve for the deflection V_D at point D

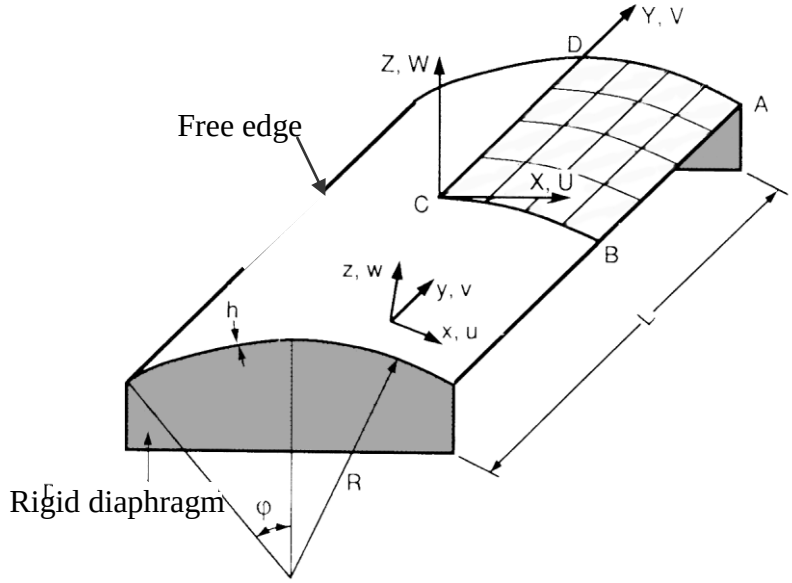

Data:

L = 6 m ; R = 3 m ; h = 0,03 m ; $\varphi = 40°$

E = 3 x 10^{10} Pa ; $\nu = 0$; f_z = -0,625 x 10^4 Pa

Boundary conditions:

$U = W = \theta_Y = 0$ for AD

Symmetry conditions:

$U = \theta_Y = \theta_Z = 0$ for CD

$V = \theta_X = \theta_Z = 0$ for CB

Reference value (Deep Shell Theory):

W_B = -3,61 cm ; W_C = 0,541 cm

Analytical solution (Shallow Shell theory):

W_B = -3,703 cm ; W_C = 0,525 cm

U_B = -1,965 cm ; V_A = -0,1513 cm

Fig.7. Scordelis-Lo roof

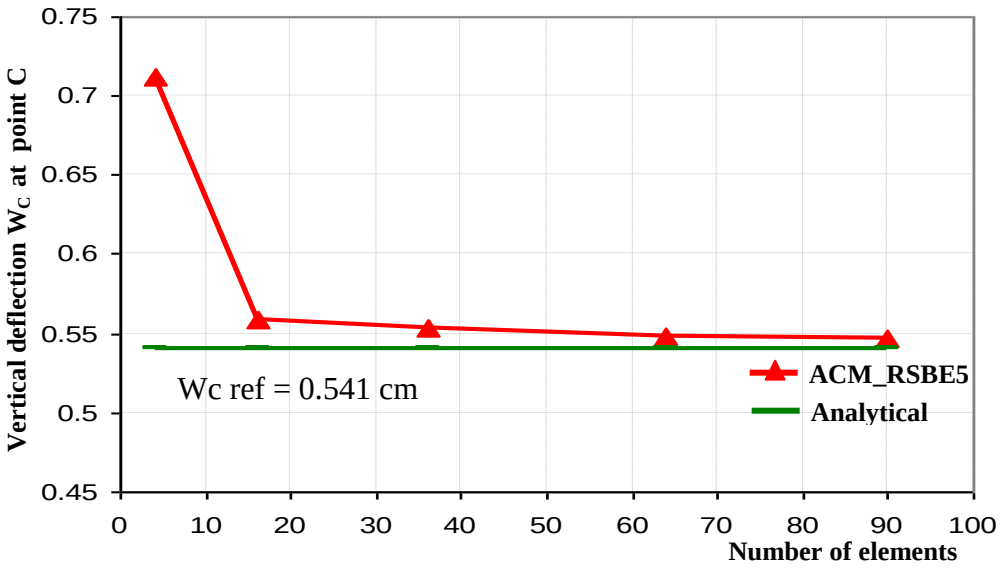

Fig.8. Convergence curve for the deflection Wc at point C for Scordelis-Lo roof

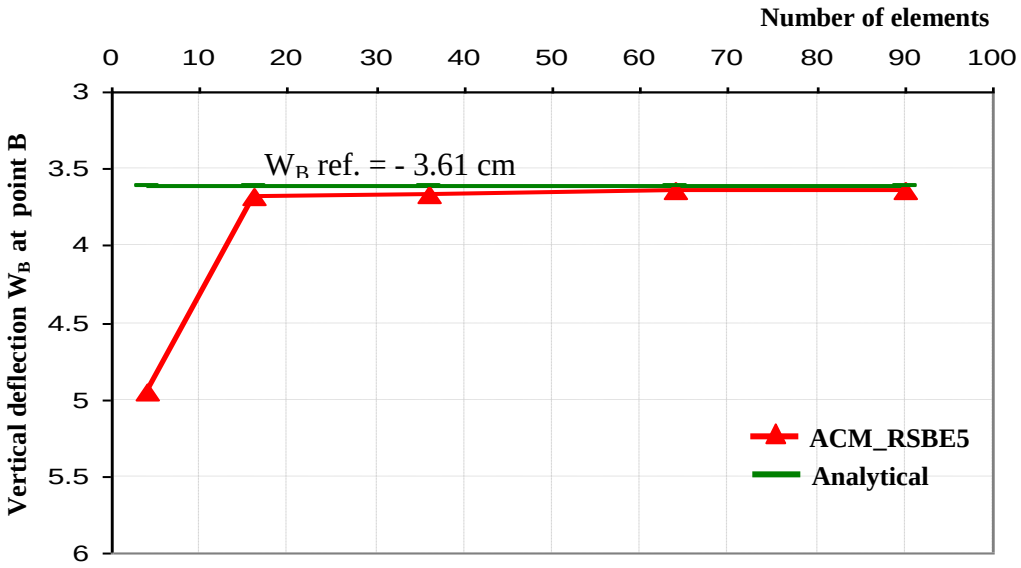

Fig.9. Convergence curve for the deflection W_B at point B for Scordelis-Lo roof

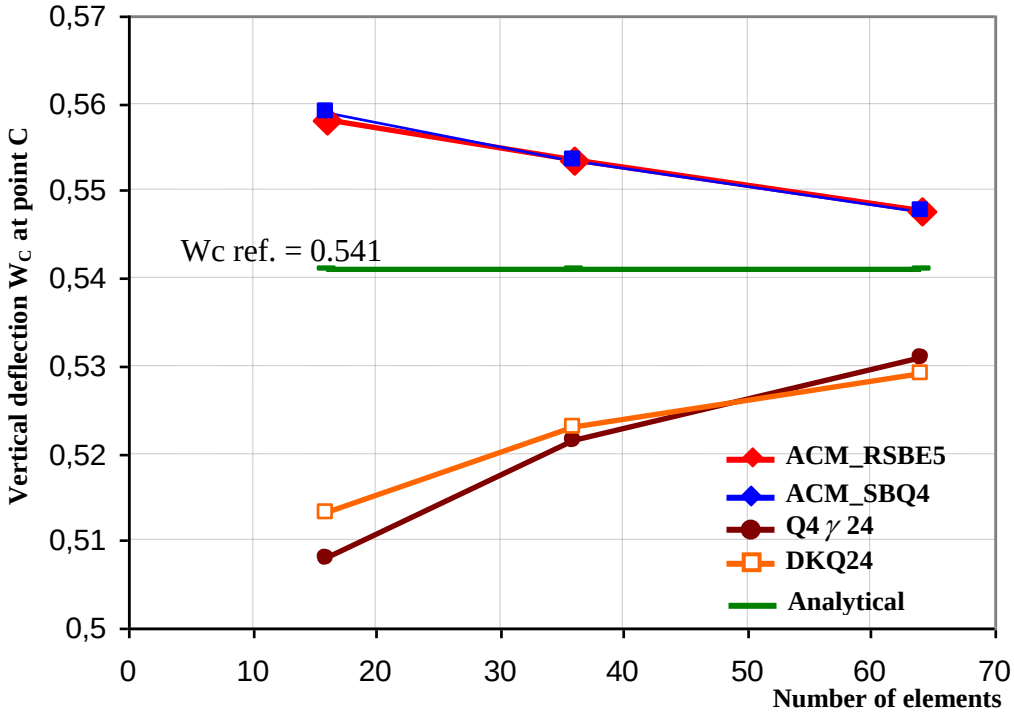

Fig.10. Convergence curve for the deflection Wc at point C for Scordelis-Lo roof

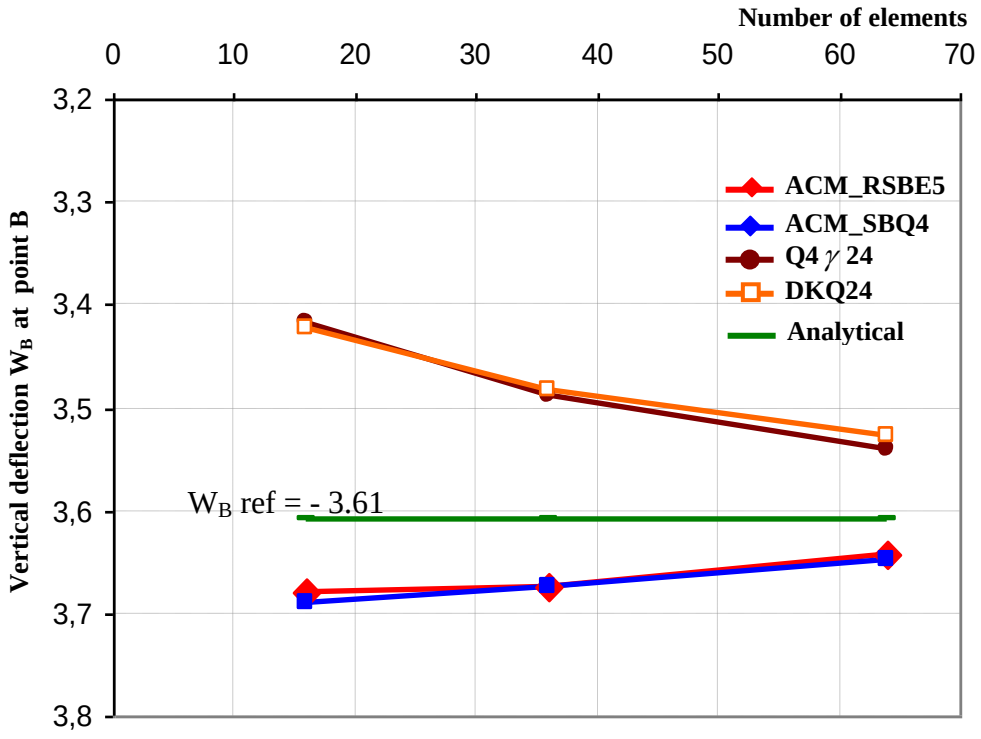

Fig.11. Convergence curve for the deflection W_B at point B for Scordelis-Lo roof

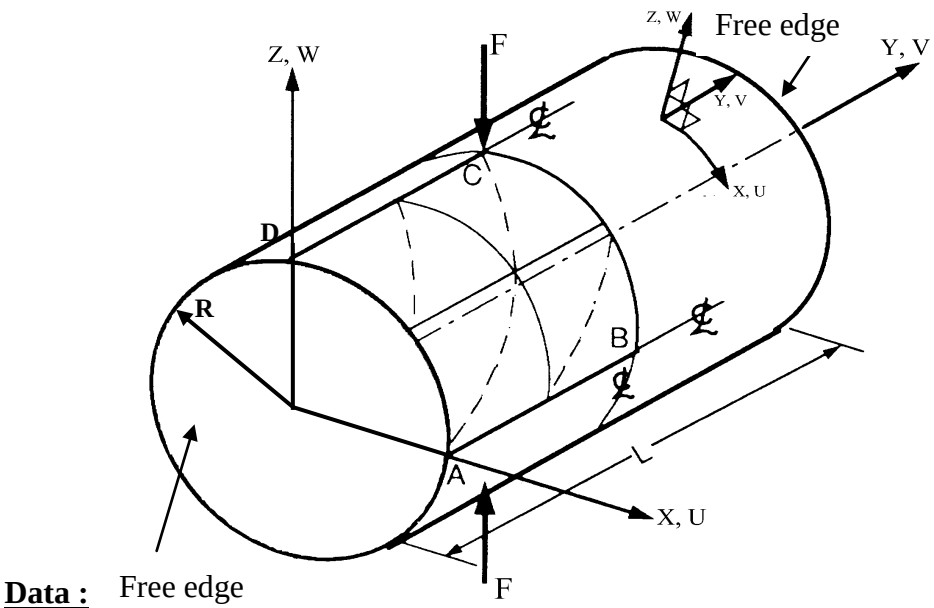

Data :

L=10,35 m ; R=4,953 m ; E=10,5 10^6 Pa ; ν=0,3125
F_1=100 KN; h_1=0,094 m; F_2=0,1 KN ; h_2=0,01548 m

Fig.12. Pinched Cylinder with free edges

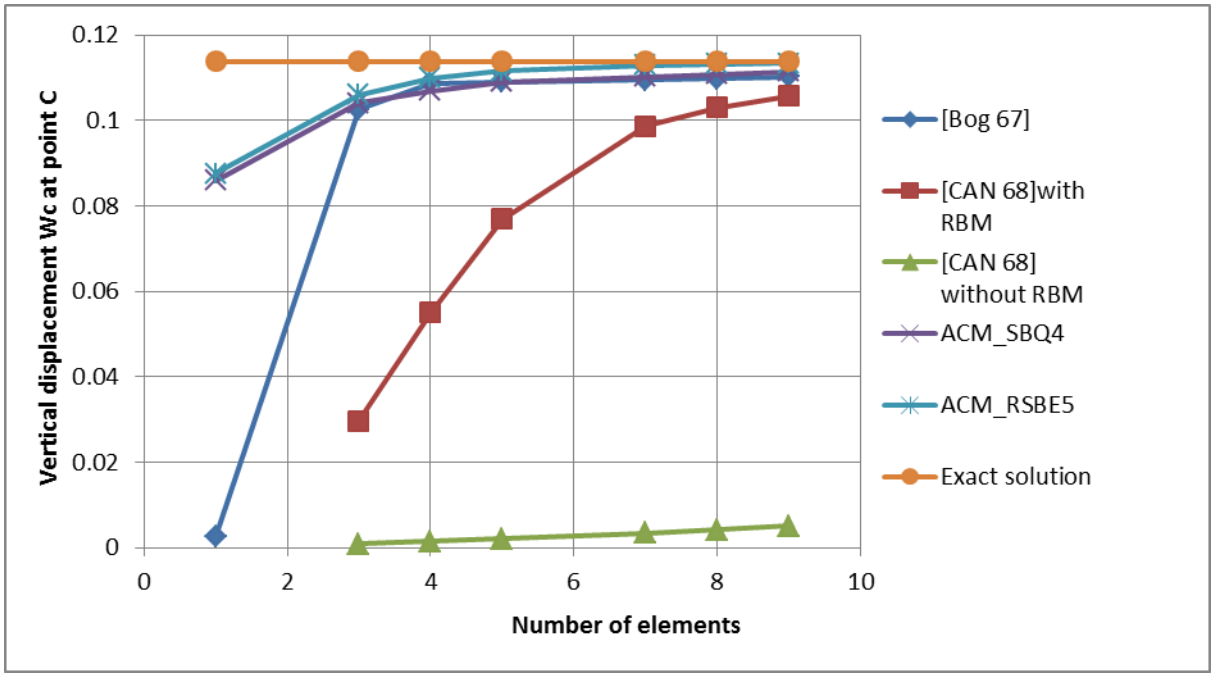

Fig.13. Convergence curve for the deflection Wc at point C for ACM_RSBE5 element and other quadrilateral shell elements, Pinched Cylinder with free edges, case 1

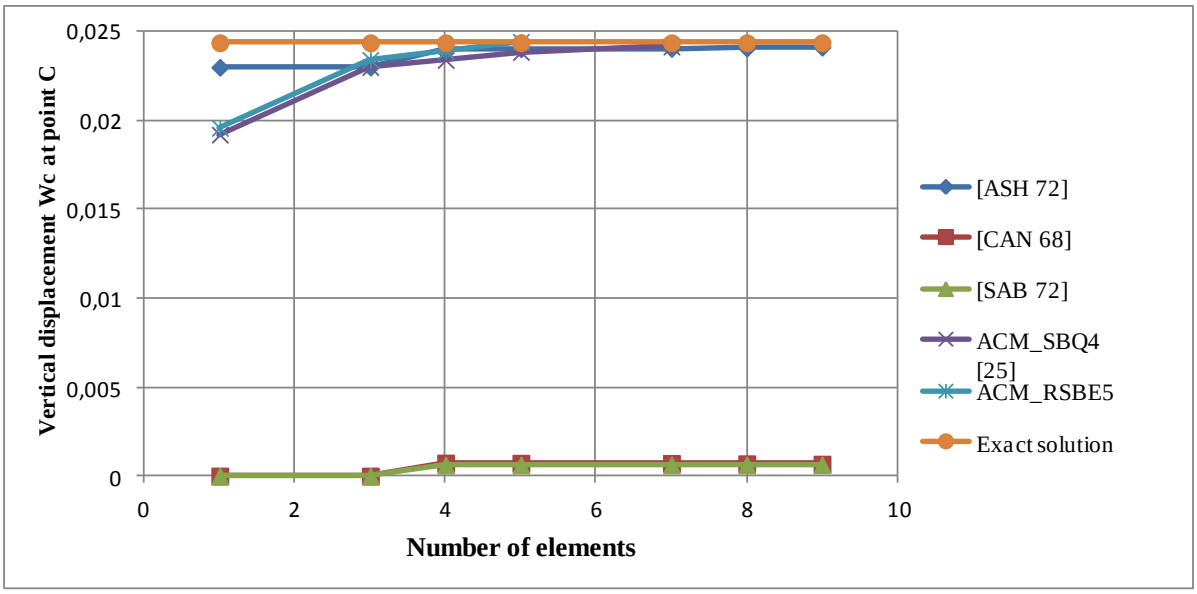

Fig.14. Convergence curve for the deflection Wc at point C for ACM_RSBE5 element and other quadrilateral shell elements, Pinched Cylinder with free edges, case 2

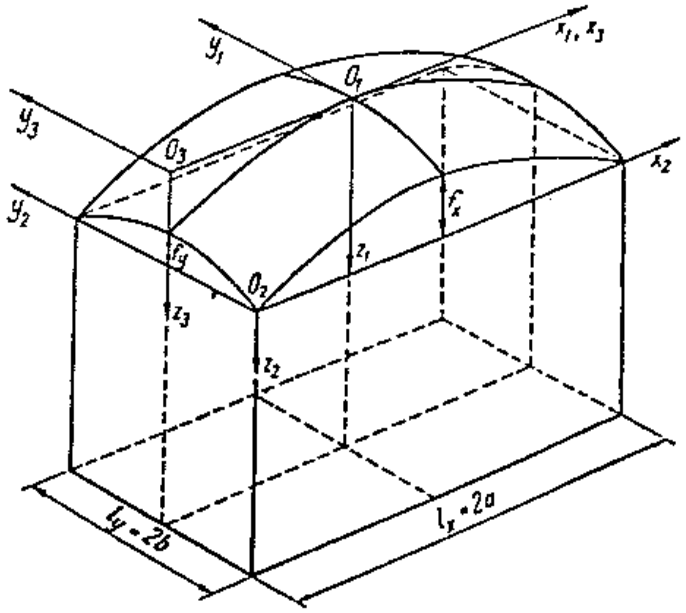

Fig.15. Elliptic paraboloid rectangular on plan

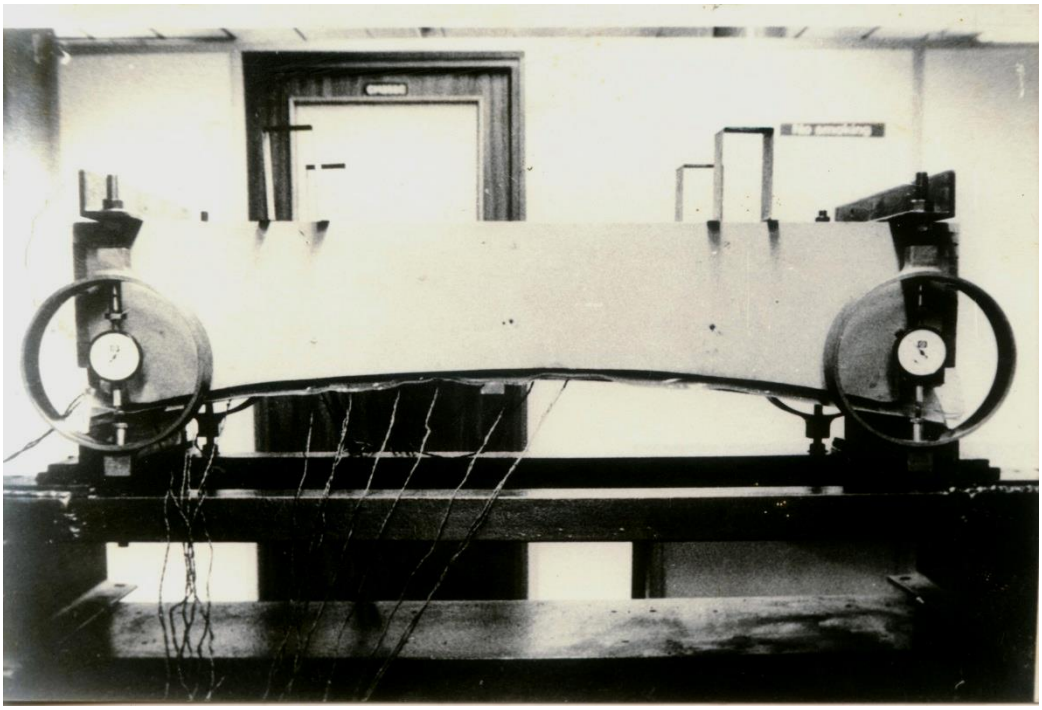

Fig.16. Elliptical paraboloid shell undergoing the experimental test

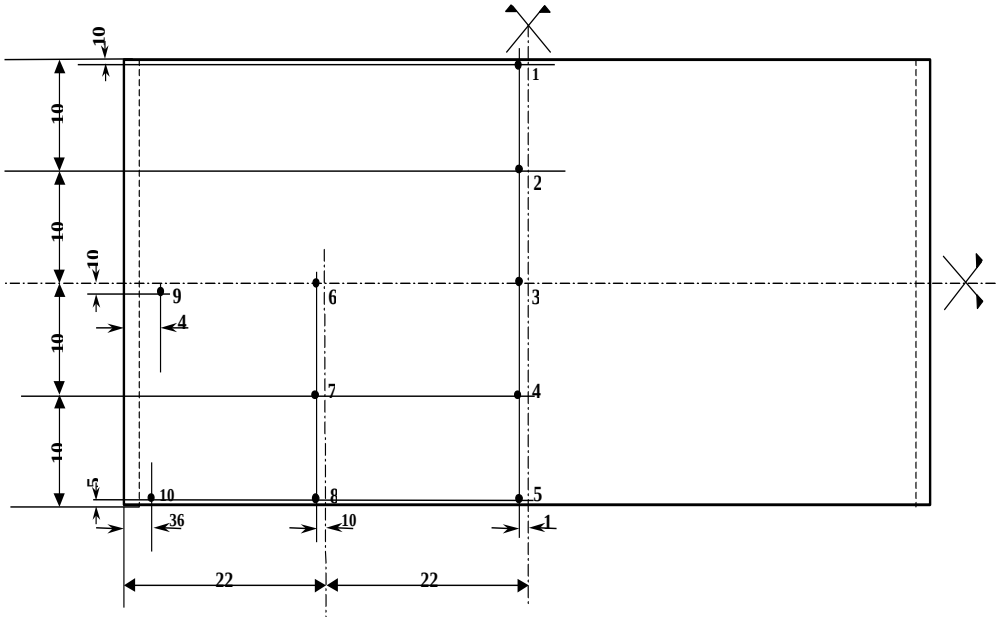

Fig.17. Dial gauge positions; (distance in mm)